

## Structural studies of pressure-induced phase transitions in selenium up to 150 GPa

Y. Akahama, M. Kobayashi, and H. Kawamura

*Department of Material Science, Faculty of Science, Himeji Institute of Technology, 1479-1 Kanaji,  
Kamigohri Hyogo 678-12, Japan*

(Received 11 June 1992; revised manuscript received 10 August 1992)

High-pressure x-ray-diffraction experiments on selenium have been carried out over a wide range of pressures up to 150 GPa and five structural phase transitions have been found: from a hexagonal-Se (Se-I) to an intermediate (Se-II) phase at 14 GPa, to a base-centered monoclinic (Se-III) phase at 23 GPa, to a base-centered orthorhombic (Se-IV) phase at 28 GPa, to a  $\beta$ -Po-type primitive rhombohedral (Se-V) phase at 60 GPa, and to a body-centered-cubic (Se-VI) phase at 140 GPa. This structural-transition sequence corresponds to a change of the system toward higher symmetry and exhibits a similarity to that of Te. These transitions are discussed from a crystallographic viewpoint.

### I. INTRODUCTION

Recently there is increasing interest in the high-pressure behavior of elemental materials and extensive studies of their structural phase transitions in the megabar-pressure regime have been carried out. The suggestion has been made<sup>1,2</sup> that elemental materials in the same group of the Periodic Table have a similar sequence of pressure-induced structural transitions.

The group-VIb elements selenium and tellurium, whose most stable form under ambient conditions is the hexagonal one with a spiral-chain structure, exhibit various structural phase transitions under high pressure. Both of these elements exhibit<sup>3,4</sup> a typical pressure-induced semiconductor-metal transition and their metallic phases become superconducting at low temperatures.<sup>5-8</sup>

Previous high-pressure structural studies of Te have shown that hexagonal Te undergoes four structural phase transitions with increasing pressure to a monoclinic phase at 4.5 GPa,<sup>9</sup> to an orthorhombic phase at 6 GPa,<sup>9</sup> to a  $\beta$ -Po-type structural phase at 11 GPa<sup>10</sup> and to the three-dimensional, higher-symmetry bcc structure at 27 GPa.<sup>11</sup> In Se, four structural transitions have been reported up to 51 GPa by Mao, Zou, and Bell<sup>12</sup> but the structures of these high-pressure phases remained unsolved. In a recent high-pressure x-ray-diffraction investigation up to 50 GPa, Parthasarathy and Holzapfel<sup>13</sup> have observed three structural phase transitions and proposed structures for these phases; however, these structures showed no similarity to those of Te and no higher-symmetry structures such as a bcc structure, was observed.

The purpose of the present study is to determine whether or not Se exhibits a similarity to Te in the structural phase-transition sequence under increasing pressure. A search for a higher-symmetry structural phase is carried out up to the megabar-pressure regime with a x-ray-diffraction experiment. It is found that hexagonal Se transforms to a high-pressure phase of  $\beta$ -Po-type primitive rhombohedral structure at 60 GPa,<sup>14</sup> and a transition from this  $\beta$ -Po-type to a bcc structure at a high pressure of about 140 GPa has been predicted. And fur-

ther, an inconsistency has arisen in the volume vs pressure relation between the present and previous data; namely, the atomic volume of the  $\beta$ -Po-type structural phase, which is the highest-pressure phase of Se, is larger than those of the lower-pressure phases at 50 GPa proposed by Parthasarathy and Holzapfel.<sup>13</sup> Therefore, a more detailed structural study on the phase transitions in the lower-pressure region for Se was required.

In the present study, results of high-pressure x-ray-diffraction experiments for hexagonal Se over a wide range of pressures up to 150 GPa are presented. A five-stage structural-phase-transition sequence from a hexagonal (Se-I) to an intermediate (Se-II) phase at 14 GPa, to a monoclinic (Se-III) phase at 23 GPa, to an orthorhombic (Se-IV) phase at 28 GPa, to a  $\beta$ -Po-type-structure (Se-V) phase at 60 GPa, and finally to a bcc (Se-VI) phase at 140 GPa is demonstrated. The Se-V to Se-VI transition, to the authors' knowledge, indicates the highest transition pressure among the previously reported pressure-induced structural transitions. A similarity in the structural-phase-transition sequence of pressure-induced phase transitions between Se and Te is confirmed. Electrical resistance and superconductivity measurements for Se up to 57 GPa have also been performed, the details of which will be described elsewhere.<sup>15</sup>

### II. EXPERIMENTAL

Hexagonal Se was prepared by crystallization from amorphous form with 99.9999% purity in high vacuum at 210°C for 20 h. A diamond anvil cell (DAC) was used for high-pressure generation. In experiments under pressures up to 100 GPa, powder sample was put into a 75  $\mu$ m diameter hole of metal gasket with both a ruby chip and a methanol:ethanol:water mixture in 16:3:1 ratio and pressurized by diamond anvils with a 150  $\mu$ m top surface. Pressure generation above 100 GPa was carried out by using diamond anvils with a central flat diameter of 75  $\mu$ m, a bevel angle of 7° and a culet diameter of 300  $\mu$ m without use of any pressure-transmitting medium. Pressure was determined by a ruby fluorescence method.<sup>16</sup>

High-pressure x-ray-diffraction experiments at room

temperature were carried out by an angle-dispersive method by using an imaging plate detector. Powder x-ray patterns at pressure above 80 GPa were obtained with use of a synchrotron radiation source (SR) on beam line 6B at the Photon Factory National Laboratory for High Energy Physics (KEK). The x-ray beam was monochromatized with a Si(111) double crystal to a wavelength of 0.68880 Å and was directed to the sample through a pinhole collimator 40 μm in diameter. A detailed description of the SR experimental system has been given elsewhere.<sup>17</sup> X-ray patterns at pressures below 80 GPa were obtained with a conventional source from a rotating-anode-type generator with a molybdenum target. A triple-pinhole collimator with pinhole diameters of 300, 70 and 90 μm was inserted in the beam path between a graphite monochromator and a DAC.

### III. RESULTS AND DISCUSSIONS

Figures 1(a) and 1(b) show the pressure dependences of the  $d$  values of diffraction lines in the lower and higher-pressure regimes, respectively. The dependences for pressures up to 150 GPa indicate five structural phase transi-

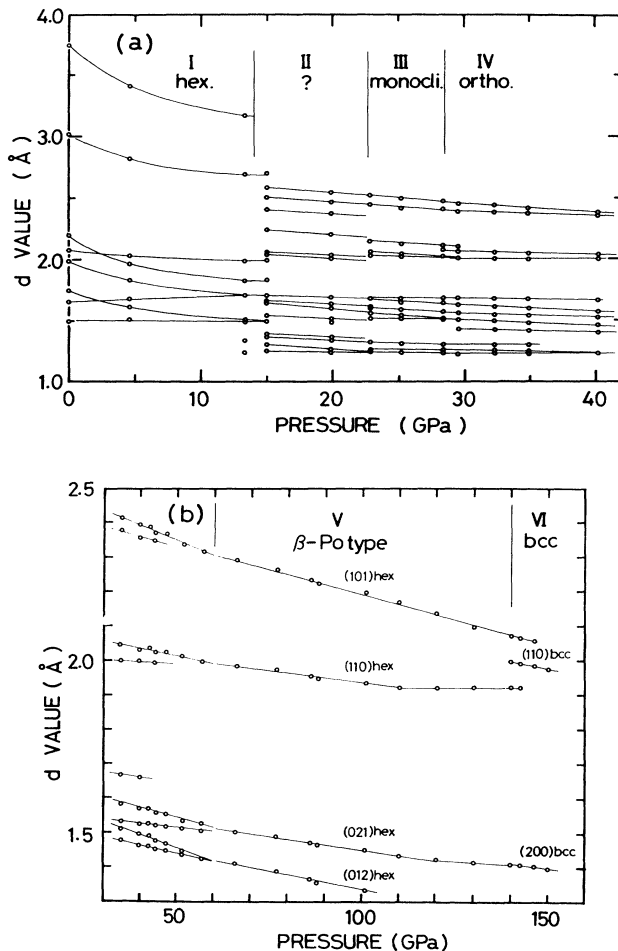


FIG. 1. Pressure dependences of the  $d$  values of diffraction lines in lower (a) and higher (b) pressure regimes.

tions: the hexagonal (Se-I)-to-intermediate (Se-II) transition at about 14 GPa, intermediate (Se-II)-to-monoclinic (Se-III) transition at 23 GPa, monoclinic (Se-III)-to-orthorhombic (Se-IV) transition at 28 GPa, orthorhombic (Se-IV)-to- $\beta$ -Po-type-structure (Se-V) transition at 60 GPa, and  $\beta$ -Po-type (Se-V)-to-bcc (Se-VI)-structure transition at about 140 GPa. The crystal-structure data at transition pressure  $P_{tr}$  for each high-pressure phase are summarized in Table I. In the present study, the transitions at 41 GPa and 51 GPa previously reported<sup>12</sup> were not observed. The results about the transitions are represented and discussed in order of increasing pressure.

#### A. Hexagonal (Se-I) -to-intermediate (Se-II) transition

A drastic change occurs in the pressure dependence of the  $d$ -values at 14 GPa [shown in Fig. 1(a)], while the Se-I phase displays a strong pressure dependence. Diffraction lines due to the Se-I phase vanish and fourteen other lines appear. This structural transition was also reported in previous studies,<sup>12,13</sup> but the diffraction pattern due to the Se-II observed in the present work differs from that obtained previously by Parthasarathy and Holzapfel.<sup>13</sup> The pattern of the present work could not be explained as a monoclinic lattice as proposed by them. The structure of the Se-II phase remains unsolved. The pressure dependence of the electrical resistance shows an anomaly around the transition pressure but a temperature dependence of the resistance in the Se-II phase is semiconductive.<sup>15</sup>

#### B. Intermediate (Se-II) -to-monoclinic (Se-III) transition

Figure 1(a) also shows the absence or appearance of diffraction lines at 23 GPa. The change corresponds to the phase transition to monoclinic structure, which phase consists of a layered structure, as will be mentioned in Sec. III C. By comparing the patterns of these three phases, it is found that the ones due to the Se-II phase resemble those due to the Se-III phase. This fact suggests that the Se-II structure is not a chainlike one-dimensional structure, but rather a layered structure. This transition was previously observed by Mao, Zou, and Bell,<sup>12</sup> but not by Parthasarathy and Holzapfel.<sup>13</sup>

The semiconductor-metal transition for hexagonal Se begins at 23 GPa.<sup>15</sup> Therefore, the metallization of Se corresponds to the structural transition to monoclinic phase in the same manner as Te. The monoclinic phase exhibits a superconducting phase transition at 26 GPa at 5.6 K.<sup>15</sup>

#### C. Monoclinic (Se-II) -to-orthorhombic (Se-IV) transition

Figures 2(a) and 2(b) show the typical diffraction patterns due to the Se-III and Se-IV phases. The pattern due to the Se-III phase was obtained in a decreasing-pressure cycle. Twelve diffraction lines for each phase are observed except for a few lines from extra phases. The patterns due to the Se-III and Se-IV phases can be explained, respectively, as a monoclinic and an orthorhombic system. Both systems satisfy the extinction rule of a base-centered space lattice,  $A^*$ . The lattice constants of the

TABLE I. Crystal-structure data at transition pressures,  $P_{tr}$ , for each high-pressure phase. Lattice constants of the Se-V phase are referred to a hexagonal lattice. The  $-\Delta V/V_0$  represents a relative volume reduction estimated at the transition pressure. Both  $d_1$  and  $d_2$  correspond to first- and second-nearest-neighbor distances, respectively.

Phase	$P_{tr}$ (GPa)	Structure	Lattice constants	Bond length	$-\Delta V/V_0$	Coordination number
I		Hexagonal	$a_H=4.366(2) \text{ \AA}$ , $V=81.78(7) \text{ \AA}^3$ $c_H=4.958(3) \text{ \AA}$ $Z=3$	$d_1=2.37 \text{ \AA}$		2 (chain)
II	14	Unknown (intermediate)				
III	23	Base-centered monoclinic	$a=4.061(1) \text{ \AA}$ , $\beta=93.33(2)$ $b=6.448(2) \text{ \AA}$ , $V=69.49(5) \text{ \AA}^3$ $c=2.658(2) \text{ \AA}$ , $Z=4$			4 (layer)
IV	28	Base-centered orthorhombic	$a=4.03(1) \text{ \AA}$ , $V=65.9(2) \text{ \AA}^3$ $b=6.22(1) \text{ \AA}$ , $Z=4$ $c=2.63(1) \text{ \AA}$		1.0%	4 (layer)
V	60	$\beta$ -Po-type primitive rhomohedral	$a_H=3.992(3) \text{ \AA}$ , $Z=3$ $c_H=3.119(2) \text{ \AA}$ $V=43.04(8) \text{ \AA}^3$	$d_1=2.53 \text{ \AA}$ $d_2=3.12 \text{ \AA}$ $d_2=3.12 \text{ \AA}$	<0.2%	6+2 (half-layer)
VI	140	bcc	$a=2.823(1) \text{ \AA}$ , $Z=2$ $V=22.49(6) \text{ \AA}^3$	$d_1=2.447 \text{ \AA}$	<0.2%	8 (cube)

base-centered monoclinic lattice at 23 GPa are  $a=4.061(3) \text{ \AA}$ ,  $b=6.447(4) \text{ \AA}$ ,  $c=2.658(2) \text{ \AA}$ ,  $\beta=93.3(3) \text{ \AA}$ , and  $V=69.4(1) \text{ \AA}^3$ ; the lattice constants of the base-centered orthorhombic lattice at 34.9 GPa are  $a=4.019(2) \text{ \AA}$ ,  $b=6.062(4) \text{ \AA}$ ,  $c=2.587(1) \text{ \AA}$ , and  $V=63.07(12) \text{ \AA}^3$ . The monoclinic lattice is quite different from that proposed by Parthasarathy and Holzapfel.<sup>13</sup> The crystal-structure data of these two phases at the transition pressure are summarized in Table I.

Figure 3 shows the pressure dependences of the lattice constants of the high-pressure phases, Se-III and Se-IV. Linear compressibilities to three crystal axis directions in both phases show a strong anisotropy. The linear compressibility,  $K$ , in the  $a$ -,  $b$ -, and  $c$ -axis directions, in average of Se-IV, are estimated to be

$K_a=4.1 \times 10^{-4}/\text{GPa}$ ,  $K_b=24 \times 10^{-4}/\text{GPa}$ , and  $K_c=11 \times 10^{-4}/\text{GPa}$ , respectively.  $K_b$  is six times as large as  $K_a$ . The strong anisotropy suggests that both the Se-III and Se-IV phase consist of a layered structure. The angle,  $\beta$ , between the  $a$ - and  $c$ - axes of the Se-III structure, which decreases with increasing pressure, discontinuously reduces to  $90^\circ$  at the transition pressure of 28 GPa. The change is recognized by the behavior of

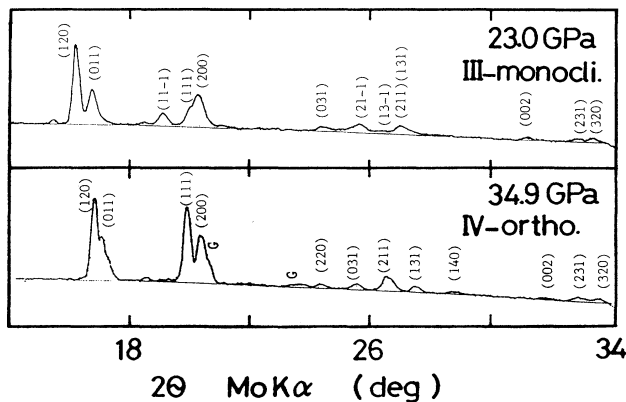


FIG. 2. Powder x-ray-diffraction patterns for the high-pressure Se-III and Se-IV phases.

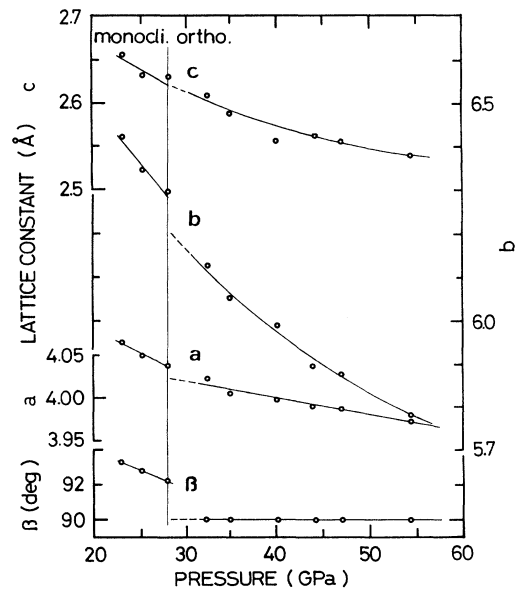


FIG. 3. Pressure dependences of lattice constants for the Se-III and Se-IV phases.

the pressure dependence of the diffraction lines in Fig. 1(a). Namely, the (111) line due to the phase appears between the (111) and (11 $\bar{1}$ ) lines due to the Se-III phase.

A model of the crystal structure for the orthorhombic (Se-IV) phase is proposed in the present study, as illustrated in Fig. 4. The structure is basically the same as the monoclinic (Te-II) phase of Te (Ref. 9) and consists of a puckered layer. Each layer is shifted alternately by a half a lattice constant along the  $c$  axis and is stacked in the  $b$ -axis direction. Atoms numbered from 1 to 8 frame a unit cell. Base center corresponds to the  $b$ - $c$  plane. The number of atoms in the unit cell  $Z$  is 4. Each atom has four nearest neighbors in the layer. The monoclinic lattice can be derived from the orthorhombic lattice by an increase in the angle  $\beta$  and has a layered structure with a coordination number of 4.

The pressure dependence of atomic volume of both phases is shown in Fig. 10 together with another phases. The volume reduction,  $-\Delta V/V_0$  ( $V_0=27.26 \text{ \AA}^3$ ), of the monoclinic-orthorhombic transition was estimated to be about 1%.

#### D. Orthorhombic (Se-IV)- to- $\beta$ -Po-type (Se-V) transition

It is found from Fig. 1(b) that the fourth structural transition occurs at 60 GPa. Though twelve diffraction lines due to the Se-IV phase were observed, the number of the line decreases to 4 at the transition pressure in a diffraction window of  $2\theta=34^\circ$ . The pressure dependences of the  $d$  values of the diffraction lines have a sharp kink at 60 GPa. This decrease in the number of diffraction lines, which is accomplished by a change from a doublet to a singlet line with a continuous narrowing in the linewidth or by a decay of the intensity, suggests that the higher-pressure phase has a higher-symmetry structure and the transition is a of second order. The (101) and (102) lines indexed for the Se-IV phase by Parthasarathy and Holzapfel<sup>13</sup> are not observed in our experiment.

A typical diffraction pattern of the high-pressure (Se-V) phase at 87.9 GPa is shown in Fig. 5. The diffraction pat-

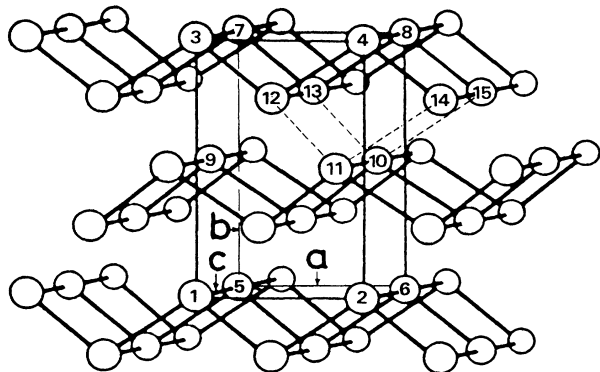


FIG. 4. A structural model for the base-centered orthorhombic lattice of the Se-IV phase. It consists of a puckered layer. The solid and broken lines show the frameworks of orthorhombic and  $\beta$ -Po-type lattices, respectively.

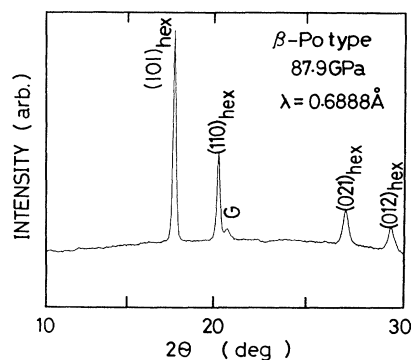


FIG. 5. Typical diffraction pattern of the Se-V phase.

tern can be interpreted as a  $\beta$ -Po-type structure of the primitive rhombohedral lattice, which is different from the rhombohedral structure proposed previously.<sup>13</sup> This  $\beta$ -Po-type structure belongs to the space group  $R\bar{3}m$ . The lattice constants at 87.9 GPa, in the hexagonal setting, are  $a=3.8920(3) \text{ \AA}$ ,  $c=2.9572(2) \text{ \AA}$ ,  $V=38.796(8) \text{ \AA}^3$  and  $Z=3$ . Each atom has six first-nearest neighbors at a distance of  $2.510 \text{ \AA}$  and two second-nearest neighbors at a distance of  $2.957 \text{ \AA}$ . The diffraction data are summarized in Table II. The scattering intensity  $I_{hkl}$  was calculated from the following formula,

$$I_{hkl} = KM_{hkl} |F_{hkl}|^2 f(\theta), \quad (1)$$

where  $K$  is the scale factor,  $M$  is the multiplicity,  $F$  is the structure factor, and  $f(\theta)$  is a function of the scattering angle,  $\theta$ , i.e., the product of polarization, Lorentz factors, and the absorption coefficient. The calculated values are in good agreement with the obtained data for both the diffraction angle and intensity.

The  $\beta$ -Po-type primitive rhombohedral lattice with a coordination number of 6 can be easily derived from the orthorhombic lattice of the Se-IV phase (shown in Fig. 5) by shortening the interlayer distance. Eight atoms of 4, 8, 10, 11, 12, 13, 14, and 15 frame a primitive rhombohedral cell when the 4-8, 4-12, and 11-12 bond distances are the same.

Figure 6 shows the pressure dependence of  $a$ ,  $c$ , and

TABLE II. Powder diffraction data for high-pressure (Se-V) phase of selenium at 87.9 GPa. X-ray wavelength  $\lambda=0.68880 \text{ \AA}$ . Rhombohedral cell:  $a=2.510 \text{ \AA}$ ,  $\alpha=104.31^\circ$ .

		Lattice constants			Space group		
		Hexagonal (rhombohedral)			$R\bar{3}m$		
		$a=3.8920(3) \text{ \AA}$					
		$c=2.9572(2) \text{ \AA}$					
		$V=38.796(8) \text{ \AA}^3$					
		$Z=3$					
$h$	$k$	$l$	$2\theta$ (obs)	$d$ (obs)	$d$ (calc)	$I$ (obs)	$I$ (calc)
1	0	1	17.8305	2.22231	2.2222	100	100
1	1	0	20.3857	1.94618	1.9462	38	68
0	2	1	27.2080	1.46422	1.4641	14	28
0	1	2	29.4687	1.35410	1.3534	12	14

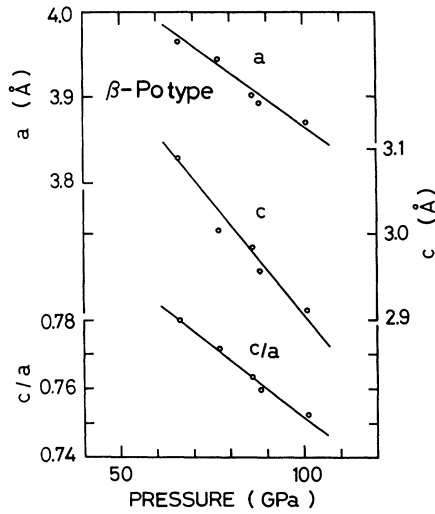


FIG. 6. Pressure dependences of lattice constants,  $a$ ,  $c$ , and  $c/a$  of the Se-V phase.

$c/a$ . The linear compressibility in the  $c$ -axis direction is about two times larger than that in the  $a$ -axis direction. The ratio  $c/a$  of 0.781 at 60 GPa decreases to 0.753 at 101 GPa with increasing pressure. The  $\beta$ -Po-type structure can be derived from both the simple-cubic structure and the bcc structure by a rhombohedral distortion along the  $[111]$  direction. In the hexagonal setting for the primitive cell, the ratio  $c/a$  of the simple-cubic structure and the bcc structure are, respectively, 1.225 and 0.612. The decrease of the ratio  $c/a$  means that the  $\beta$ -Po-type structure progresses to the bcc structure with increasing pressure. By analogy to Te, the transition pressure from the  $\beta$ -Po type to the bcc structure is estimated to be 140 GPa.

The pressure dependence of atomic volume is plotted in Fig. 10 together with previous data by Parthasarathy and Holzapfel.<sup>13</sup> The Se-V structure has the reduced volume,  $V/V_0$  of 0.53 at 60 GPa, which decreases to 0.46 at 101 GPa. Our data for each high-pressure phase are consistent with one another in the volume vs pressure relation. On the contrary, the previously reported values<sup>13</sup> are considerably smaller compared with the present data.

#### E. $\beta$ -Po-type (Se-V) -to-bcc (Se-VI) transition

Figure 7 displays diffraction patterns obtained at different pressures. In the bottom most pattern at 101 GPa, which arises from the Se-V phase, the reflection indices are referred to those of a hexagonal lattice. At 140 GPa, one can clearly see an appearance of one additional peak between  $(101)_{\text{hex}}$  and  $(110)_{\text{hex}}$ . At 150 GPa, the diffraction peaks from the Se-V phase completely vanish and only two diffraction peaks remain within a half-angle window,  $2\theta=31^\circ$ . Two other peaks can be assigned to  $(110)_{\text{bcc}}$  and  $(200)_{\text{bcc}}$  based on the body-centered-cubic (bcc) lattice. The intensity ratio between the  $(110)_{\text{bcc}}$  and  $(200)_{\text{bcc}}$  can be satisfactorily explained by the bcc Bravais lattice shown in Fig. 8. Therefore, these facts clearly

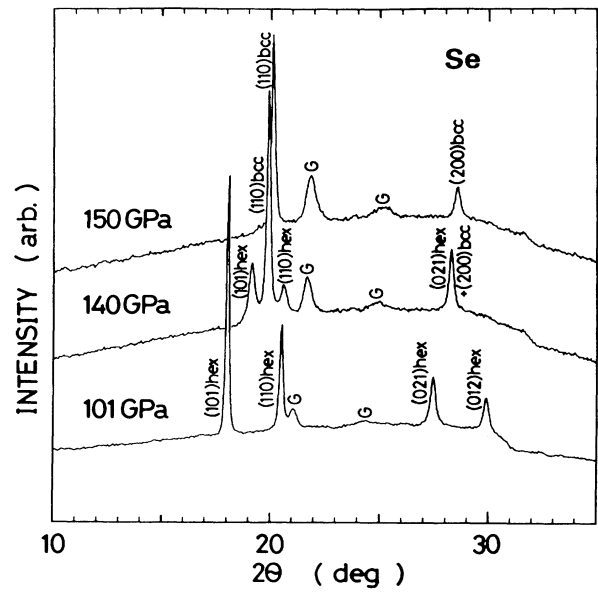


FIG. 7. Diffraction patterns at various pressures: 101, 140, and 150 GPa.

show the presence of the bcc (Se-VI) phase at about 140 GPa.

The  $d$  spacing around the transition is also shown in Fig. 1(b). The lattice constants of the Se-V phase were determined from the  $(101)_{\text{hex}}$ ,  $(110)_{\text{hex}}$ , and  $(021)_{\text{hex}}$  by a least-squares method and those of the Se-VI phase was determined from  $(110)_{\text{bcc}}$ .

Next, we discuss this transition from a crystallographical viewpoint based on a rhombohedral distortion. A  $\beta$ -Po-type primitive rhombohedral lattice can be derived from a bcc Bravais lattice by a rhombohedral distortion along the  $[111]$  direction as shown in Fig. 8. The  $[111]$  distortion leads to a decrease in the rhombohedral angle  $\alpha_R$  ( $109.28^\circ$  for the bcc lattice) and results in a change in the atomic configuration from a coordination number of 8 to a coordination by 6 first-nearest neighbors and 2 second-nearest neighbors. In terms of the rhombohedral lattice constants,  $a_R$ , and  $\alpha_R$ , the hexagonal lattice constants,  $a_H$  and  $c_H$ , are given by

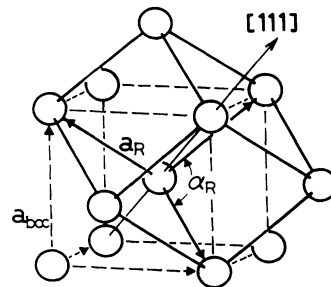


FIG. 8. A  $\beta$ -Po-type primitive rhombohedral lattice of Se, which derives from a bcc lattice by a rhombohedral distortion. The solid and broken lines show the frameworks of the rhombohedral and  $\beta$ -Po-type lattices, respectively.

$$a_H = 2a_R \sin(\alpha_R/2), \quad (2)$$

$$c_H/a_H = [9/4 \sin^2(\alpha_R/2) - 3]^{1/2}. \quad (3)$$

The ratio  $c_H/a_H$  indicates the magnitude of the [111] distortion. When the system is distortion free, this ratio is equal to 0.612. The ratio  $c_H/a_H$  decreases from 0.785 to 0.753 with increasing pressure from 60 to 101 GPa. The fact means a relaxation of the distortion. We predicted that the  $\beta$ -Po-type-bcc transition is accomplished around 140 GPa because this transition takes place in Te with a ratio  $c_H/a_H$  of about 0.72.<sup>11</sup> Therefore, we consider the present results as successful observation of such a transition taking place at about 140 GPa, as predicted.

The  $\beta$ -Po-type lattice is also described by the first-nearest neighbor distance,  $d_1$ , and the second-nearest neighbor distance,  $d_2$ .  $d_1$  and  $d_2$  correspond to lattice constants,  $a_R$  and  $c_H$ , respectively. In Fig. 9(a), the pres-

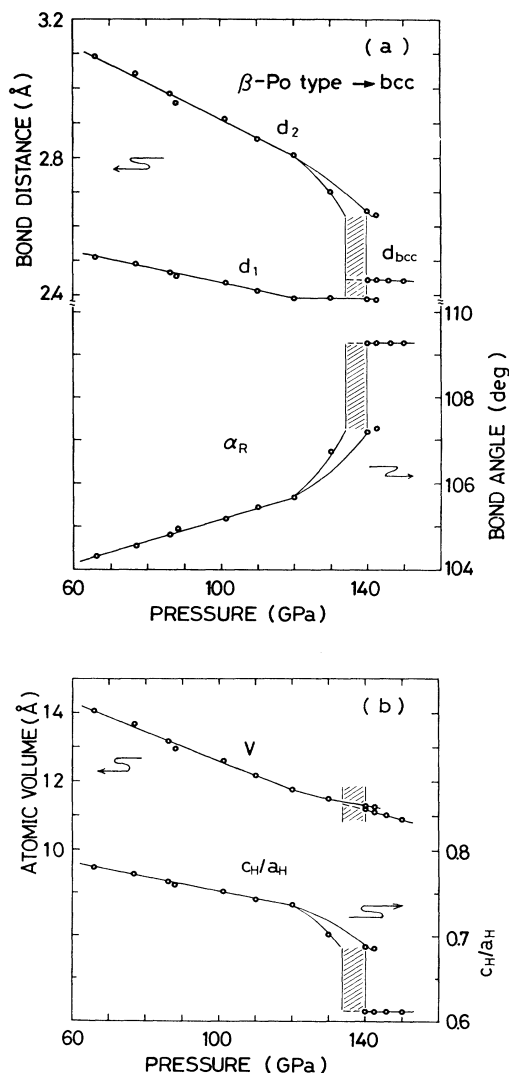


FIG. 9. Pressure dependences of  $d_1$ ,  $d_2$ , and  $\alpha_R$ (a) and the atomic volume  $V$ , and the ratio  $c_H/a_H$ (b) for the Se-V and Se-VI phases.

sure dependences of the bond distances  $d_1$  and  $d_2$  and the rhombohedral angle  $\alpha_R$  are plotted. At the transition from the Se-V to the Se-VI phase,  $d_1$  and  $d_2$  meet discontinuously and change into the first-nearest neighbor distance of the bcc lattice,  $d_{\text{bcc}}$ . The bond distance  $d_1$  elongates by 2.3%, while  $d_2$  contracts by 7.5%. The discontinuous change leads to an increase in  $\alpha_R$  from 107.2° to 109.28°. This behavior is reasonable in view of the general tendency shown by covalent solids in which a pressure-induced breakdown of directional bonds and an increase in the coordination number result in an increase in  $d_1$ . In the higher-pressure phase, the atomic coordination number becomes 8. The value of  $d_{\text{bcc}}$  at 150 GPa is 2.4189(3) Å and is longer by 2.1% compared with the bond length 2.37 Å for the Se-I phase under ambient pressure.

One should note the pressure dependences of  $d_1$ ,  $d_2$ , and  $\alpha_R$  in the Se-VI phase. These parameters show a linear pressure dependence in the lower-pressure regime. A positive pressure coefficient of  $\alpha_R$ , 0.025 deg/GPa, means a monotonical relaxation of the [111] distortion. But under pressures above 120 GPa, a hardening in  $d_1$  and a softening in  $d_2$  occur simultaneously. Consequently,  $\alpha_R$  rapidly increases. This means the acceleration of relaxation in the distortion. If this behavior corresponds to a precursor phenomenon of this transition, it is suggested that it may be a second-order transition. As shown in Fig. 9(b), this behavior also makes the ratio  $c_H/a_H$  shift to 0.69 at the transition point from the value of 0.72, which was estimated by analogy to Te.<sup>11</sup>

The pressure dependences of the atomic volume for the Se-V and Se-VI phases are shown in Fig. 9(b). The estimated relative volume reduction is less than 0.2% at 140 GPa. It is considerably smaller than the value of 2.0% in the transition of Te.<sup>11</sup> We should note that the coexistence of both the Se-V and Se-VI phases results from an inhomogeneity in the sample pressure due to the absence of a pressure-transmitting medium. In Fig. 10,

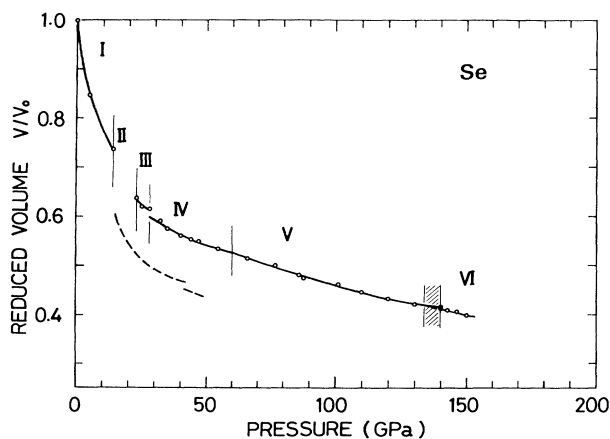


FIG. 10. Pressure dependence of the reduced volume  $V/V_0$  for each high-pressure phase of Se. The broken lines show the previously reported data of Parthasarathy and Holzapfel (Ref. 13).

the dependence of the Se-VI phase, when combined with our data, does not lead to any contradictions in the volume vs pressure relation. At 150 GPa, the atomic volume reaches 40% of the original volume at atmospheric pressure.

#### IV. CONCLUSION

In the present study, five structural phase transitions in Se were confirmed for pressures up to 150 GPa and the structures of four of these high-pressure modifications were determined. As a result, the structural-phase-transition sequence hexagonal (Se-I) –intermediate (Se-II)–monoclinic (Se-III)–orthorhombic (Se-IV) – $\beta$ -Po-type (Se-V)–bcc to (Se-VI) was revealed. This sequence exhibits a similarity to that of Te, as expected. The

structural transitions correspond to a change of the system toward higher symmetry. In other works, these were transformations from a spiral-chain structure to a puckered-layered structure, than to higher-symmetry layered structure, and finally to a cubic structure and they were accompanied by a systematic increase in the coordination number: 2 (Se-I)–? (Se-II)–4 (Se-III)–4 (Se-IV)–6 (Se-V)–8 (Se-VI). A discussion from a crystallographical viewpoint has also been carried out of these transitions.

#### ACKNOWLEDGMENTS

The authors would like to thank Dr. K. Takemura and Dr. H. Fujihisa for their cooperation in setting up the experimental system and analysis of diffraction data at the Photon Factory.

<sup>1</sup>A. K. McMahan, *Physica* **139&140B**, 31 (1986).

<sup>2</sup>H. L. Skriver, *Phys. Rev. B* **31**, 1909 (1985).

<sup>3</sup>F. P. Bundy and K. J. Dunn, *J. Chem. Phys.* **71**, 1550 (1979).

<sup>4</sup>P. W. Bridgman, *Proc. Am. Acad. Arts Sci.* **81**, 167 (1952).

<sup>5</sup>J. Wittig, *Phys. Rev. Lett.* **15**, 159 (1965).

<sup>6</sup>F. P. Bundy and K. J. Dunn, *Phys. Rev. B* **22**, 3157 (1980).

<sup>7</sup>I. V. Berman, Zh. I. Binzarov, and P. Kurkin, *Fiz. Tverd. Tela* **14**, 2527 (1972) [*Sov. Phys. Solid State* **14**, 2192 (1973)].

<sup>8</sup>F. P. Bundy and K. J. Dunn, *Phys. Rev. Lett.* **44**, 1623 (1980).

<sup>9</sup>K. Aoki, O. Shimomura, and S. Minomura, *J. Phys. Soc. Jpn.* **48**, 551 (1980).

<sup>10</sup>J. C. Jamieson and D. B. McWhan, *J. Chem. Phys.* **43**, 1149 (1965).

<sup>11</sup>G. Parthasarathy and W. B. Holzapfel, *Phys. Rev. B* **37**, 8499

(1988).

<sup>12</sup>H. K. Mao, G. Zou, and P. M. Bell, *Carnegie Inst. Washington Yearb.* **80**, 283 (1980).

<sup>13</sup>G. Parthasarathy and W. B. Holzapfel, *Phys. Rev. B* **38**, 10105 (1988).

<sup>14</sup>Y. Akahama, M. Kobayashi, and H. Kawamura, *Solid State Commun.* **83**, 269 (1992); **83**, 273 (1992).

<sup>15</sup>Y. Akahama, M. Kobayashi, and H. Kawamura (unpublished).

<sup>16</sup>H. K. Mao, P. M. Bell, J. W. Shaner, and D. J. Steinberg, *J. Appl. Phys.* **49**, 3276 (1978).

<sup>17</sup>O. Shimomura, K. Takemura, H. Fujihisa, Y. Fujii, T. Kikegawa, Y. Amemiya, and T. Matsusita, *Rev. Sci. Instrum.* **63**, 967 (1992).